Lawrence Berkeley National Laboratory
LBL Publications

Title
Advanced Hydrogen-Bromine Flow Batteries with Improved Efficiency, Durability and Cost

Permalink
https://escholarship.org/uc/item/48w3j0g3

Journal
Journal of The Electrochemical Society, 163(1)

ISSN
0013-4651

Authors
Lin, G
Chong, PY
Yarlagadda, V
et al.

Publication Date
2016

DOI
10.1149/2.0071601jes

Peer reviewed

Advanced Hydrogen-Bromine Flow Batteries with Improved Efficiency, Durability and Cost

G. Lin [a,*, z], P.Y. Chong [a], V. Yarlagadda [b] and T.V. Nguyen [b, **], R.J. Wycisk [c,*] and P.N. Pintauro [c,**], M. Bates [d] and S. Mukerjee [d, **], M.C. Tucker [e] and A.Z. Weber [e *]

[a] TVN Systems, Inc.
Lawrence, KS 66046, USA

[b] Department of Chemical and Petroleum Engineering
The University of Kansas, Lawrence, KS 66045, USA

[c] Department of Chemical and Biomolecular Engineering
Vanderbilt University, Nashville, TN 37235, USA

[d] Department of Chemistry and Chemical Biology
Northeastern University, Boston, MA 02115, USA

[e] Environmental Energy Technologies Division
Lawrence Berkeley National Laboratory, Berkeley, CA 94720, USA

[*] Electrochemical Society Active Member.
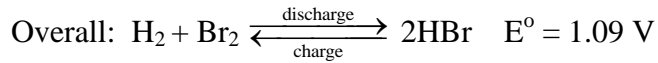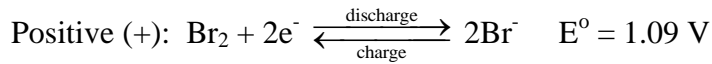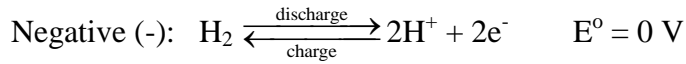[**] Electrochemical Society Fellow.
[z] Corresponding Author, E-mail: gygylin@gmail.com

Abstract

The hydrogen/bromine flow battery is a promising candidate for large-scale energy storage due to fast kinetics, highly reversible reactions and low chemical costs. However, today's conventional hydrogen/bromine flow batteries use membrane materials (such as Nafion®), platinum catalysts, and carbon-paper electrode materials that are expensive. In addition, platinum catalysts can be poisoned and corroded when exposed to HBr and Br_2, compromising system lifetime. To reduce the cost and increase the durability of H_2/Br_2 flow batteries, new materials are developed. The new Nafion/ polyvinylidene fluoride electrospun composite membranes have high perm-selectivity at a fraction of the cost of Nafion membranes; the new nitrogen-functionalized platinum-iridium catalyst possesses excellent activity and durability in HBr/Br_2 environment; and the new carbon-nanotube-based Br_2 electrodes can achieve equal or better performance with less materials when compared to baseline electrode materials. Preliminary cost analysis shows that the new materials reduce H_2/Br_2 flow-battery energy-storage system stack and system costs significantly. The resulting advanced H_2/Br_2 flow batteries offer high power, high efficiency, substantially increased durability, and expected reduced cost.

1. Introduction

The Hydrogen/Bromine (H_2/Br_2) flow battery is a potential large-scale energy storage device because of its numerous advantages such as rapid Br_2 and H_2 reaction kinetics, low cost, and abundance of the active materials used.[1-7] The charge and discharge reactions occurring are as follows:

Negative (-): $H_2 \underset{\text{charge}}{\overset{\text{discharge}}{\rightleftharpoons}} 2H^+ + 2e^-$ $E^o = 0$ V

Positive (+): $Br_2 + 2e^- \underset{\text{charge}}{\overset{\text{discharge}}{\rightleftharpoons}} 2Br^-$ $E^o = 1.09$ V

Overall: $H_2 + Br_2 \underset{\text{charge}}{\overset{\text{discharge}}{\rightleftharpoons}} 2HBr$ $E^o = 1.09$ V

The active reactant material, hydrobromic acid (HBr) is also used as the supporting electrolyte. If the energy-storage system is commissioned in the discharged state, which is the most common case, HBr is the only chemical that is required. During charge, hydrobromic acid is electrolyzed to generate hydrogen and bromine, which are stored in separate tanks. Bromine has a moderate solubility in water which can be greatly enhanced by the presence of Br^- via complexation to form Br_3^- or Br_5^-.[8,9] The gas phase H_2 electrode also simplifies the separation and recovery of crossover catholyte, which can be returned back to the catholyte tank.

The H_2/Br_2 flow battery technology has been under investigation since the 1960s. Brief literature reviews can be found in recent publications by Cho *et al.* [4], Kreutzer *et al.*[5] and Tolmachev.[6] H_2/Br_2 flow batteries share the same cell architecture as proton-exchange-membrane fuel cells (PEMFCs). Therefore, H_2/Br_2 flow batteries are also referred to as regenerative or reversible H_2/Br_2 fuel cells. Similar to PEMFCs, membrane-electrode assemblies (MEAs) are the most crucial components in the H_2/Br_2 flow batteries. In today's state-of-the-art

H_2/Br_2 flow batteries, MEAs are commonly made of commercial perfluorosulfonic acid (PFSA) membranes such as Nafion®, platinum catalysts, and plain carbon papers.

The PFSA membrane in a H_2/Br_2 flow battery is used to physically separate the positive and negative electrodes, and prevent mixing of hydrogen and bromine/bromides while allowing proton transport between the electrodes. The membrane resistance has a large impact on the flow-cell performance. The resistance can be lowered by reducing membrane thickness or implementing pretreatment procedures, such as boiling in water, which notably increases the cell power density by improving membrane conductivity.[4,5,10] However, both approaches also increase the crossover rate of bromine species (i.e. bromine and bromide ions) across the membrane, leading to reduced coulombic efficiency, especially at lower operating current.[11] The crossover of catholyte through the membrane also requires the return of liquid back to the solution tank, which adds system complexity and operation cost. A more severe issue is that the presence of bromine-species at the negative side adversely impacts the H_2 electrode catalyst. Hydrogen oxidation/evolution reactions (HOR/HER) at the negative side require noble-metal catalysts such as platinum, which is not stable in the HBr/Br_2 environment and is known to be susceptible to bromide adsorption and corrosion leading to reduced catalyst lifetime.[12-15] In contrast to the H_2 reactions, the bromine reactions do not require noble-metal catalysts at the positive electrode. Carbon is a suitable electrode material because of facile bromine reaction kinetics and excellent stability in HBr/Br_2 environment. Due to the high viscosity of aqueous HBr/Br_2 solution and the use of interdigitated flow fields, porous gas-diffusion media (GDM) are used to ensure the liquid electrolyte penetrates the carbon electrode at reasonable pressure drop. Three to four layers of GDM are used to provide sufficient active area for the Br_2 reaction, due to the low surface area of commercial GDM.[4]

For any technology to be economically viable for large-scale energy storage, cost and durability must be addressed. The H_2/Br_2 flow-battery system has cost advantages when compared to all-vanadium flow-battery systems (e.g, \$400 /kW-h [10] versus \$800 /kW-h [16] for a 4-hour discharge duration). However, cost must be reduced and durability must be increased further for this technology to be cost effective. Therefore, this work focuses on the development of low-cost and durable improved MEA materials. The performance of new materials in H_2/Br_2 flow cells is reported along with preliminary cost analysis.

PFSA membranes have been long recognized as one of the most expensive components in PEMFC and flow-battery stacks. New types of low-cost membranes such as nanoporous proton conducting membranes (NP-PCM) composed of polyvinylidene fluoride (PVDF) with silica [3] and nano-fiber Nafion/PVDF electrospun composite membranes have been developed *via* dual fiber electrospinning.[17] While the NP-PCM with 60% porosity exhibited low cost and good performance, the authors also acknowledge the high liquid flux across the membrane. Nafion/PVDF electrospun composite membranes demonstrated reduced membrane swelling and bromine/bromides permeation. In addition, less Nafion ionomer material would be needed for the composite so a lower membrane cost is expected according to a preliminary cost analysis for a Nafion/polyphenylsulfone composite membrane developed for H_2/air fuel cells.[18]   Following these results, this work develops highly selective nanofiber-based Nafion/PVDF composite membranes for the H_2/Br_2 flow battery *via* a single-fiber electrospinning process which is simpler and more cost-effective than the dual-fiber electrospinning process. [19]

Since no membrane can completely block Br_2/Br^- crossover, platinum poisoning/corrosion still occurs at the negative side. A cathodic protection strategy is commonly used to prevent corrosion by ensuring a constant supply of hydrogen to the negative

electrode.[13,20] However, in an *in-situ* test under continuous H_2 gas protection, Cho *et al.* reported a Pt loss of 2.6% after 230 cycles over seven days in 1M HBr solution.[13] In a more recent cycling test, the H_2 electrode charge-transfer resistance increased considerably after 3164 hours continuous cycling, suggesting a loss of active surface area.[11] During the lifetime of an energy-storage system, interruption of H_2 gas supply to the negative electrode may occur. For example, in the case of H_2 pump failure, H_2 gas flow through the negative side is interrupted while HBr/Br_2 solution continues to cross through the membrane and accumulate in the H_2 electrode. The electrode can become saturated with HBr/Br_2 solution, leading to a complete loss of Pt activity. Therefore, the durability of H_2 catalysts in H_2/Br_2 flow batteries is a major factor limiting system lifetime. Thus, a goal of this work is to develop a new catalyst with increased durability in concentrated HBr/Br_2 electrolytes.

Lastly, the use of multiple layers of expensive carbon paper as the Br_2 electrode proves costly. The ionic diffusion distance also increases due to the increased Br_2 electrode thickness, which adversely affects cell performance.[21] In this work, we attempt to enhance the surface area of plain carbon GDM by growing carbon nanotubes directly on GDM substrates. It was previously suggested that this cost-effective approach would minimally impact the morphological properties (porosity and tortuosity) of the carbon GDM, while improving the active surface area.[22]

2. Experimental

Fabrication of Nafion/PVDF composite membranes. – Single-nanofiber mats were prepared by electrospinning solutions containing mixtures of 1100 EW Nafion PFSA and polyvinylidene fluoride. The raw mats were post-processed into dense membranes by hot pressing at 177°C, followed by thermal annealing at 150°C. A single-layer membrane was fabricated using one

solution with Nafion/PVDF weight ratio of 80/20. A tri-layer membrane was also fabricated by successively electrospinning Nafion/PVDF (90/10) solution, then Nafion/PVDF (60/40) solution, and finally Nafion/PVDF (90/10) solution. The mat was then processed and converted to a tri-layer composite membrane by hotpressing and annealing as described above. The nanofiber membranes were boiled in 1 M sulfuric acid and deionized water (one hour for each boiling step) to ensure full protonation of the sulfonic acid sites. The membranes were then dried in ambient conditions. The overall PVDF contents were 20 wt% and 13 wt% for the single-layer and tri-layer composite membranes, respectively.

Synthesis of nitrogen-functionalized platinum-iridium catalyst – The nitrogen-functionalized platinum-iridium catalyst (Pt-Ir-N_x) supported on high surface-area carbon black (Pt-Ir-N_x/C) was synthesized via a simple solvo-chemical method, modified from the development of Pt-N_x/C described by Oh and Kim.[23]   In short, the platinum and iridium chloride salts were dispersed in water followed by the addition of a nitrogen complexing agent (1,3-propylenediamine) and finally addition of the carbon black support. The reactants were stirred at room temperature overnight, during which time the nitrogen-complexed metals absorbed into the pores of the high surface-area carbon support. The resulting solid product was filtered, washed, dried in a vacuum-oven and then annealed in a tube furnace at 700°C under an inert argon atmosphere. The resulting Pt-Ir-N_x/C catalyst had a Pt:Ir atomic ratio of 1:1 and 40 wt% of metal on carbon support.

Synthesis of CNT based carbon electrodes. – Carbon nanotubes (CNTs) were synthesized directly on the carbon electrode fiber surface. SGL Sigracet carbon paper GDL-10AA was used as the substrate (also referred to as plain GDL). The synthesis of CNT-based electrodes involved two major steps. First, a pulse current electrodeposition process was used to deposit cobalt (Co)

nanoparticles onto the carbon surface. This process was conducted with a three electrode arrangement in a solution containing cobalt sulfate ($CoSO_4$) and boric acid (H_3BO_3). The deposited Co nanoparticles catalyzed the growth of multi-walled CNTs during the second step: chemical vapor deposition in the presence of acetylene (C_2H_2), argon (Ar), and hydrogen (H_2) gas mixture at high temperature. The synthesized CNT electrodes were sonicated in de-ionized (DI) water for 30 minutes and subsequently soaked in 1M nitric acid (HNO_3) overnight to etch away the exposed Co metal nanoparticles. The DI water sonication gets rid of any amorphous carbon and other impurities present in the carbon electrode. The detailed synthesis process can be found in reference [22].

Flow cell polarization performance measurement. – The new composite membranes, H_2 catalysts and Br_2 electrodes were assembled and evaluated in 1-cm^2 flow cells. An interdigitated graphite flow field plate was used on the H_2 side with a flow field area of 1 cm by 1 cm. A tantalum plate was used on the Br_2 side with two parallel channels 1 cm long and 1 cm apart. H_2 and Br_2 electrodes (1.2 cm by 1.2 cm and 1 cm by 1.2 cm, respectively) slightly bigger than the flow area were used to prevent gas/liquid shortcut between channels and an effective active area of 1.2 cm^2 was used in the current density calculation. Conventional MEAs made of baseline materials - Nafion NR212 (Ion Power), Pt/C (60wt%, Tanaka) and Sigracet GDL 10AA carbon paper (SGL Group) – were also tested to obtain baseline performance for comparison. Then each baseline material was substituted with new corresponding material, and the MEA was tested under the same conditions (fresh materials were used in each test). H_2 electrodes were prepared by coating catalysts onto Sigracet GDL-25BC and then hot-pressed (135°C, 1.5MPa, 5mins) onto pure Nafion or composite membranes to form half-MEAs. Half-MEAs with Nafion membranes were subsequently boiled in DI water for one hour to increase the membrane conductivity, and

then stored in DI water at room temperature prior to testing. No additional pretreatment was done on half-MEAs with Nafion/PVDF composite membranes. Both plain and CNT bromine electrodes were pretreated by boiling in DI water for one hour and then soaked and stored in 99.9% H_2SO_4 at room temperature to improve their wetting characteristics and active area prior to flow cell testing. An aqueous solution of HBr/Br_2 was recirculated through the Br_2 electrode. The solution volume was 2 liters for 2M HBr/0.9M Br_2 solution and 3.5 liters for 1M HBr/0.9M Br_2 so the concentration variation and loss of solution due to crossover were negligible during each polarization scan. After each scan, solutions were brought back to initial state-of-charge (SOC) by charging/discharging the cell at constant voltage to equalize the discharge/charge capacities (amp-hour). Humidified H_2 gas at a flow rate of 30-40 mL/min flowed through the H_2 electrode and vented out at ambient pressure. Various flowrates of HBr/Br_2 solution were used and specified along with other test conditions and material pre-treatments in the results and discussion section. All the flow cell experiments were conducted at room temperature unless otherwise specified.

Polarization curves were obtained using an Arbin MSTAT4 potentiostat/galvanostat and MIT Pro data acquisition software. MEAs were subjected to an initial break-in process by using current-control staircase discharge/charge cycling mode (0.1 A/cm^2 and 30s per step, with cutoff voltages of 0.2 V/1.4 V). Then the step-size was changed to 50 mA/cm^2 and the cell was cycled another 2 to 3 times until reproducible cell performance was achieved. AC impedance was measured at open circuit using a Gamry Interface 1000 (Br_2 electrode as working electrode, H_2 electrode as counter/reference electrode, 5 mV perturbation amplitude, 0.2Hz-100kHz, 20 points/decade).

Pt-Ir-Nx catalyst evaluation in H₂ - pump cell. – The HOR/HER activities of the new Pt-Ir-Nx/C catalyst and standard Pt/C catalyst were also evaluated in a 5-cm^2 H$_2$ -pump cell with serpentine flow-fields according to the protocols in reference [5]. A Pt gas-diffusion electrode with a loading of 0.35 mg Pt/cm^2 was used as the reference and counter electrodes, and a Pt-Ir-N$_x$/C or Pt/C (0.35 mg-metal/cm^2) electrode was used as the working electrode. The electrodes were hot-pressed onto commercial Nafion 212 membranes. The cell was operated at room temperature (~23°C) with a H$_2$ flow rate of 500 mL/min at 100% relative humidity to both the anode and cathode under 124 kPa absolute backpressure. Polarization performance was obtained with current-staircase mode and high-frequency resistance was measured at open circuit and used for iR correction.

Energy efficiency, crossover and self-discharge rate measurement. – Energy efficiency, water and bromine-species crossover rate and self-discharge rate were measured in a 10-cm^2 flow cell using a Biologic VMP-3 potentiostat. Membranes and H$_2$ electrodes were not hotpressed, and the detailed setup and cell configuration can be found in reference [11], and protocols in reference [10]. Crossover rate for bromine-species was determined by collecting the liquid exiting the H$_2$ exhaust. The exit line was cooled to 0.5 ^{o}C to condense water and bromine vapor. The collected liquid was then analyzed for bromide content using a bromide-selective electrode, with the electrode and Reference Sensor (DX200 and DX280, Mettler Toledo) connected to an ORION 4 STAR datalogger (Thermo SCIENTIFIC). Electrolytes (1 M KNO$_3$ and 3 M KCl) and ionic strength adapter (5 M sodium nitrate) were provided by Mettler Toledo. Sodium bromide (99.7%, ACS Reactant, J. T. Baker) dried for 2 h at 120 ^{o}C in an environmental chamber (VWR Symphony) was used as a calibration standard. All measurements were performed at room temperature. Self-discharge rate was determined by cycling the cell from 0.5 to 1.2 V at 75 mA/

cm^2 and calculated as the difference between charge and discharge capacity per cell area divided by the cycle time.

Cell cycling. – Cell cycling was conducted with the same 10-cm^2 flow cell in battery mode (closed catholyte and hydrogen loops). A glass reservoir held hydrogen that was circulated through the cell and returned to the reservoir through a liquid trap. The liquid accumulated in the reservoir was pumped to the catholyte tank several times per charge/discharge cycle, at a rate selected to match the average crossover flux. The hydrogen tank was held at roughly ~136 kPa absolute pressure, and the pressure fluctuated slightly during charging and discharging; excess hydrogen was used to minimize the pressure variation. Cell polarization performance was assessment before and after cycling with the hydrogen exhaust vented rather than circulated.

3. Results and Discussion

3.1 Nafion/PVDF electrospun composite membranes

Most ionomer membranes, including Nafion, swell in water and aqueous HBr solutions, decreasing their anion barrier property and increasing the crossover rate of bromine-species through the membrane. The incorporation of an uncharged PVDF reinforcement improves the mechanical characteristics of the membranes and thus restricts the swelling of the ionic pathways within the ionomer. As a result, the composite membrane crossover rate is reduced and perm-selectivity is increased. The incorporation of uncharged reinforcement unavoidably reduces the membrane conductivity. However, the sheet resistance (membrane thickness divided by membrane conductivity) can be controlled by varying membrane thickness and Nafion:PVDF ratio while maintaining desired mechanical strength and crossover rate.

The synthesized single-fiber single-layer Nafion/PVDF membranes were about 30 μm thick and composed of 80 wt% Nafion and 20 wt% PVDF. For PFSA membranes there is a tradeoff between power density (membrane resistance) and coulombic efficiency (bromine-species crossover). Within a range of pre-boiled Nafion membranes, NR212 membrane (55 μm thick) was found to exhibit a reasonable tradeoff between power and energy efficiency and thus this commercially-available membrane was chosen as a baseline for comparison to the new composite membranes developed here.[11] Membrane pre-treatment has a large impact on membrane conductivity and Br-species crossover rate.[11] Therefore, NR212 membranes as-received, boiled, and boiled then air-dried were tested for comparison. The last pretreatment is chosen to mimic the processing of the Nafion/PVDF composite membrane: after hotpressing the raw mats, the composite membranes were boiled in sulfuric acid solution and DI water to remove residual carriers and to re-protonate all of the ion-exchange sites, and then air-dried prior to testing.

As shown in Figure 1a, the cell performance of boiled NR212 membrane is much higher than that of the as-received NR212 membrane, due to reduced membrane resistance as shown in Figure 1b. However, the Br-species crossover rate is increased 4-fold and self-discharge rate over 7-fold as shown in Table 1, leading to drastically decreased coulombic efficiency (Figure 1c). The energy efficiency was reduced to a maximum of 0.75 (at 250 mA/cm^2). This illustrates the tradeoff between crossover and resistance, which leads to a compromise between maximizing power or efficiency. The new Nafion/PVDF electrospun composite membrane exhibited the same or better polarization performance than the highest-conductivity NR212 (boiled) membrane as shown in Figure 1a due to the reduced sheet resistance (Figure 1b) yielding high power density. In addition, the Br-species crossover rate and self-discharge rate were nearly the same as

the lowest-crossover NR212 (as-received) membrane (Table 1). As a notable result, the energy efficiency for the new membrane is higher than NR212, either boiled or as-received, over a very wide range of current density (75 to 750 mA cm^{-2}) and exceeds 0.8 at 400 mA/cm^2 (Figure 1c). This is similar to the energy efficiency achieved for boiled and dried NR212, however significantly lower cost is projected for the composite membrane as discussed below.

3.2 Nitrogen-functionalized platinum-iridium catalyst on carbon support (Pt-Ir-N$_x$/C)

Pt-Ir-N$_x$ catalysts were tested in both a H$_2$-pump cell and a H$_2$/Br$_2$ flow cell and the iR-corrected performance is shown in Figure 2. Performance of a platinum electrode is shown for comparison. Note that the non-zero OCV of the H$_2$-pump cell was caused by slight H$_2$ gas pressure difference between the cathode and anode gas streams. In the H$_2$-pump cell, the Pt-Ir-N$_x$/C sample exhibited improved HOR activity and nearly identical HER activity when compared to that of the standard Pt/C catalyst, whereas in the H$_2$/Br$_2$ the flow cell, the Pt-Ir-N$_x$/C showed performance identical to Pt up to 1 A/cm^2 even with a lower metal loading. The lower performance beyond 1 A/cm^2 may be attributed to the un-optimized catalyst and electrode structures.

To evaluate the Pt-Ir-N$_x$/C catalyst durability, the catholyte was introduced into the negative side of the flow cell thereby soaking the H$_2$ electrode for various periods of time (see Figure 3). This is considered to be a worst-case condition for the H$_2$ electrode. At the end of soaking, dry nitrogen was flowed into the cell for 10 to 20 minutes to flush out the solution. Polarization performance and AC impedance were then re-assessed with hydrogen flow, followed by subsequent soakings. To ensure performance degradation was not caused by electrode flooding, an interdigitated flow field was used at the H$_2$ side and multiple scans were conducted to obtain reproducible performance data. For comparison, a Pt electrode was tested

under the same conditions. The results are shown in Figures 4 and 5. After each soaking, both cells with Pt and Pt-Ir-N_x catalysts exhibited decreased OCV near zero. A short pulse of charge voltage (1.25V for 5 seconds) was then applied to the cells. The Pt electrode OCV recovered partially after each early soaking but did not recover after cumulative 17-hour soaking. After only one hour of soaking, the cell with Pt electrode exhibited negligible discharge power (Figure 4a) and drastically increased H_2 electrode charge-transfer resistance (Figure 5a). In contrast, the cell OCV with Pt-Ir-N_x catalyst recovered fully after each soaking and persisted through 366 hours of cumulative soaking. AC impedance in Figure 5b shows a small gradual increase in H_2 electrode resistance in stark contrast to the large increase observed for Pt. Figure 4a shows that after soaking the cell for 18 hours, the charge performance changed very little and the discharge performance was nearly unchanged within the current range of 0 to 0.5 A/cm^2 (normal operation range for high efficiency). Although the Pt-Ir-N_x/C catalyst is not entirely immune to bromide/bromine adsorption and corrosion, the maximum power from the Pt-Ir-N_x catalyst was still about 0.58 W/mg-metal after 366 cumulative hours of soaking. This is a significant improvement over the Pt catalyst, which failed after one-hour soaking.

3.3 Carbon Nanotube (CNT) based Br$_2$ Electrodes

Performance of the new single-layer CNT electrode and the baseline electrode (a stack of three layers of pre-treated plain SGL GDL 10AA carbon paper) was determined with 2M HBr/0.9M Br$_2$ solution. It was found in a separate experiment that the baseline Br$_2$ electrode requires a solution flowrate of at least 10 mL/min/cm^2 to achieve optimal performance, and this flowrate was used here. The single-layer CNT electrode was tested with various flowrates (see Figure 6). The durability of the CNT material was also evaluated and it was found that the active carbon surface area decreased upon contact with HBr/Br$_2$ solution flow, presumably due to loss

14

of CNTs, but stabilized after about 4 hours (not shown). The test results presented here were collected beyond that 4h duration and multiple scans were conducted to obtain reproducible and steady-state performance data.

The discharge performance up to 0.7 A/cm^2 for the single-layer CNT electrode at a flowrate of 2 mL/min/cm^2 was nearly the same as the three-layer baseline material at 10 mL/min/cm^2. In addition to providing sufficient active surface area for the bromine reaction, the single-layer CNT electrode also reduces the mass-transport distance from the flow field to the membrane since its thickness is only one-third of the baseline electrode. The deviation from baseline performance at higher current may be attributed to mass-transport overpotential during discharge and a high concentration of Br$_2$ at the reaction sites during charge. Once the solution flowrate was increased from 2 to 5 mL/min/cm^2, both the charge and the discharge performance were immediately improved and surpassed the baseline material. A further increase in flowrate to 10 mL/min/cm^2 led to marginally improved performance at higher currents. Therefore, a flow rate of 5 mL/min/cm^2 would be an optimal operation point. The results demonstrate that when using CNT electrodes, equal or better performance can be achieved with less material. One may be concerned that the pressure drop across the Br$_2$ electrode may increase due to the reduced electrode thickness when compared to the three-layer baseline materials. While this is a valid concern, lower flowrates are needed to achieve equal or better performance (2 or 5 versus 10 mL/min/cm^2 for CNT and baseline materials, respectively), and proper interdigitated flow-field design can reduce the pressure drop further.

3.4 Cycling test

A Nafion/PVDF electrospun composite membrane and Pt-Ir-N$_x$ H$_2$ electrode were assembled into a 10-cm^2 flow cell and subjected to a week-long cycling test. For the cycling test

the electrospun single-fiber tri-layer Nafion/PVDF membrane with 13 wt% overall PVDF content was used. The H_2 electrode was prepared by coating Pt-Ir-N_x/C catalyst ink onto a SGL GDL 10BC with a loading of 0.5 mg-metal/cm^2. Due to the design of the flow field, which was not optimized for one-layer CNT Br_2 electrode, a baseline (+) electrode was used in this cycling test to avoid excessive pressure drop.

The cell was assessed for initial performance with 2M HBr/0.9M Br_2 solution and then cycled 100 times at a current density of 400 mA/cm^2 with cutoff voltages of 0.5/1.15V. Cell performance was re-assessed after cycling (Figure 7). The small change in discharge performance may arise from increased bromide adsorption arising from Pt or membrane permeability evolution, or small experimental deviations in bromine/bromide ratio, bromine concentration, or hydrogen pressure/flowrate as these are known to impact high-current discharge performance.[7] The capacity was very stable with an average 95% coulombic efficiency throughout the cycling test. The spikes arise from fluctuations in the syringe pump recirculating rate returning the solution accumulated at the H_2 exhaust back to the catholyte bottle. After cycling, identical charge performance was maintained and minimal degradation was observed in the discharge performance. The voltaic efficiency was somewhat lower than 0.7 due to the un-optimized tri-layer composite membrane. Nevertheless, the new materials have demonstrated excellent stability in the cycling test. Note that this cycling test was about one week long while flow batteries are expected to operate for many years, thus long-term durability tests will be conducted to further evaluate the durability of the new materials. This cell was also assessed for its performance with 1M HBr/0.9M Br_2. It was ~~also~~ noticed that this cell performed similar to the baseline materials when using 1M HBr/0.9 M Br_2 solution, but somewhat <u>the performance</u> ~~worse~~

with 2M HBr/0.9M Br_2 solution was worse than that of the baseline materials. The cause of this concentration-dependent performance will be investigated in future studies.

3.5 Preliminary cost analysis

Researchers at Lawrence Berkeley National Lab (LBNL) and Robert Bosch Corporation developed a cost model for a H_2/Br_2 flow-battery energy-storage system (hereinafter referred to as the LBNL system model).[10] In their cost model, commercial materials are assumed for the MEAs: Nafion membrane, Pt catalyst for negative electrode, plain carbon paper for positive electrode and H_2 electrode GDM. Below we estimate the costs of the new materials developed in this work and use these to replace the cost of conventional MEAs in the LBNL system model (the commercial H_2 electrode GDM remains unchanged). Refer to reference [10] for detailed model description and assumptions.

3.5.1 Cost of new MEA materials

Nafion/PVDF composite membranes - The composite membrane consists of 80 wt% Nafion and 20 wt% PVDF with a thickness of 30 μm. The membrane cost includes Nafion ionomer, PVDF polymer, and solvent material costs and manufacturing process cost (electrospinning/hotpressing/annealing). The Nafion ionomer price was reported with respect to annual purchase volume by Directed Technologies, Inc.[24]   To allow a price calculation according to the price quote at low purchase volume, a production rate of 2500 m^2/year was assumed and the ionomer cost is about $2700/kg. The average cost of PVDF is about $25/kg based on listing prices on www.alibaba.com. The manufacturing cost was estimated to be $9/$m^2$ based on the quote provided by eSpin Technologies (Chattanooga, TN). The solvent mixture costs about $3/$m^2$ and can be captured and recycled. Therefore, the estimated composite membrane cost is $140/$m^2$. Because of the incorporation of mechanically strong, uncharged

PVDF polymer, the composite membrane can be made thinner, and with a lesser amount of expensive PFSA ionomer, resulting in a cost competitive membrane compared to Nafion NR212 ($350/m^2).[25]

Pt-Ir-Nx/C catalysts – The atomic ratio of Pt:Ir is 1:1 and it can be reasonably assumed that the cost of noble metals dominates the final catalyst cost. The monthly highest prices in the last five years, $1800/oz for Pt and $1085/oz for Ir, are used to estimate the cost of Pt-Ir-Nx/C.[26] The resulting cost of new catalyst is about $1442.5/oz which is marginally less expensive than Pt. The activity is similar to Pt catalyst in H_2-Br_2 flow cells, so a loading of 0.05 mg-metal/cm^2 is assumed to be consistent with the Pt loading used in the system model, resulting in a catalyst cost of $23/m^2 (active area).

CNT Br$_2$ electrodes - The CNT Br_2 electrode cost was estimated based on the costs of plain carbon-paper substrate and other materials used in the electrodeposition and chemical-vapor-deposition processes.[27,28] It was found that the cost of one layer of CNT on 10AA electrode is about 50% of the three-layer plain 10AA baseline carbon electrode. The baseline Br_2 electrode cost was reported to be $70/m^2, [10] and a CNT Br_2 electrode is about $35/m^2. Because of the ~ 20x surface-area enhancement, a thinner CNT electrode provides sufficient active surface area for the Br_2 reaction, enabling further cost reduction.

3.5.2 Cost of new MEAs and System

The cost of MEAs with new materials is compared to conventional MEA materials in Table 2. By using the new materials, the MEA cost is reduced 47%. The new MEA cost was then entered into the LBNL system model with an area-specific resistance (ASR) of 0.27 ohm-cm^2 extracted from the experimental data. H_2/Br_2 flow-battery system cost consists of fuel-cell stack, balance-of-plant (BOP), and assembly costs. Figure 8 and Figure 9 show the system capital cost

and the breakdown of the stack cost. For comparison, the system cost with conventional materials is also shown (Gen 3 performance with ASR=0.32 ohm-cm^2 for boiled NR212 membrane taken from reference [10]). The system cost ($/kW-h) is reduced using the new materials (about 17% reduction at 1-hr discharge duration). The cost reduction results primarily from the lower stack cost (~38% reduction at 1-hr discharge duration) and the change of BOP and assembly costs is negligible. The most expensive component in the stack with conventional MEAs is PFSA membrane, which accounts for 38%. The membrane cost is reduced to 21% in the stack with new MEAs because of the low PFSA content in the composite membranes. The second most expensive component, bipolar plates, becomes the top one in the stack with new MEAs and accounts for almost half of the total stack cost due to the expensive metal coating and low production volume. Less expensive and compatible materials in addition to high production volume are expected to reduce the cost.

4. Conclusion

New MEA materials were developed for H_2/Br_2 flow batteries and evaluated in flow cells. The electrospun composite membranes made of Nafion and PVDF were able to deliver high power density while restricting the crossover of bromine and bromides, yielding high energy efficiency; the use of strong and less expensive PVDF polymers renders a significant reduction in membrane cost. The new Pt-Ir-N_x/C catalyst exhibited excellent HOR/HER activities and remarkable resistance to attack from bromine and bromides, and outperformed the durability of commercial Pt/C catalyst materials. One layer of carbon-nanotube (CNT) based Br_2 electrode material costs about 50% less than the three-layer of baseline material and provided equal or better performance at lower solution flowrates. Preliminary cost analysis showed that the new

materials reduced the MEA cost by 47% and stack and system costs by 38% and 17%, respectively, without compromising performance or durability.

Acknowledgement

References

1. W. Glass and G. H. Boyle, *Advances in chemistry series*, **47**, 203 (1965).

2. R. S. Yeo and D. T. Chin, *J. Electrochem. Soc.*, **127**(3), 549 (1980).

3. V. Livshits, A. Ulus and E. Peled, *Electrochemistry communications*, **8**, 1358 (2006).

4. K. T. Cho, P. Ridgeway, A. Z. Weber, S. Haussener, V. Battagalia, and V. Srinivasan, *J. Electrochem. Soc.*, **159**(11), A1806 (2012).

5. H. Kreutzer, V. Yarlagadda, and T. V. Nguyen, *J. Electrochem Soc.*, **159**(7), F331 (2012).

6. Y.V. Tolmachev, *Russian J. Electrochemistry*, **50**(4), 301 (2014).

7. M.C. Tucker, K.T. Cho, A.Z. Weber, G. Lin and T.V. Nguyen, *Journal of Applied Electrochemistry*, **45**, 11 (2015)

8. H. A. Liebhafsky, *J. Am. Chem. Soc.*, **56**, 1500 (1934).

9. R. S. Yeo, J. McBreen, *J. Electrochem. Soc.*, **126**, 1682 (1979).

10. K.T. Cho, P. Albertus, V. Battaglia, A. Kojic, V. Srinivasan, A. Z. Weber, *Energy Technol*, **1**, 596 (2013)

11. M. C. Tucker, K. T. Cho, F. B. Spingler, A. Z. Weber, G. Lin, *Journal of Power Sources*, **284**, 212 (2015).

12. T. V. Nguyen, H. Kreutzer, V. Yarlagadda, E. McFarland, and N. Singh, *ECS Transactions*, **53** (7), 75 (2013).

13. K. T. Cho, M. C. Tucker, M. Ding, P. Ridgway, V. S. Battaglia, V. Srinivasan, and A. Z. Weber, *ChemPlusChem*, **79**, 1 (2014).

14. M. Goor-Dar, N. Travitsky and E. Peled, *J Power Sources*, **197,** 111 (2012).

15. E. Peled, A. Blum, and M. Goor-Dar, "Hydrogen-Bromine Fuel Cells," in *Encyclopedia of Electrochemical Power Sources*, J. Garche, C. Dyer, P. Moseley, Z. Ogumi, D. Rand, and B. Scrosati, Editors, , Vol. 3, Amsterdam, Elsevier, pp. 182 (2009).

16. M. Zhang, M. Moore, J. S. Watson, T. A. Zawodzinski and R. M. Counce, *J. Electrochem. Soc.*, **159** (8), A1183 (2012)

17. J. W. Park, R. Wycisk, P. N. Pintauro, *Journal of Membrane Science*, **490**, 103 (2015).

18. P. N. Pintauro and P. T. Mather, "NanoCapillary Network Proton Conducting Membranes for High Temperature Hydrogen/Air Fuel Cells", May 2011, http://www.hydrogen.energy.gov/pdfs/review11/ fc038_pintauro_2011_o.pdf

19. R. Wycisk, J. W. Park, D. Powers, and P. N. Pintauro, "Electrospinning PFSA + PVDF Nanofibers for Fuel Cell Membrane Fabrication" Abstract #1199, ECS 226 Meeting, Cancun, Mexico, October 5-9, 2014.

20. G. G. Barna, S. N. Frank, T. H. Teherani, and L. D. Weedon, *J. Electrochem. Soc.*, **131**, 1973 (1984).

21. V. Yarlagadda and T. V. Nguyen, *J. Electrochem Soc.*, **160**(6), F535 (2013).

22. V. Yarlagadda and T. V. Nguyen, *ECS Trans*., **58**(36), 25 (2014).

23. J.-G. Oh, and H. Kim, *Journal of Power Sources*, **181**(1), 74 (2008).

24. B. D. James, J. A. Kalinoski and K. N. Baum, *Mass Production cost Estimation for Direct H2 PEM Fuel Cell Systems for Automotive Applications: 2010 Update*, Directed Technologies, Inc., September 30, 2010

25. Vanadium Redox Flow Batteries: An In-Depth Analysis. EPRI, Palo Alto, CA: 2007. 1014836

26. http://www.platinum.matthey.com/prices/price-charts

27. http://www.icis.com/chemicals/channel-info-chemicals-a-z/

28. http://bgs.vermont.gov/sites/bgs/files/pdfs/purchasing/Airgas-Price-List.pdf

Table Caption

Table 1. Membrane properties

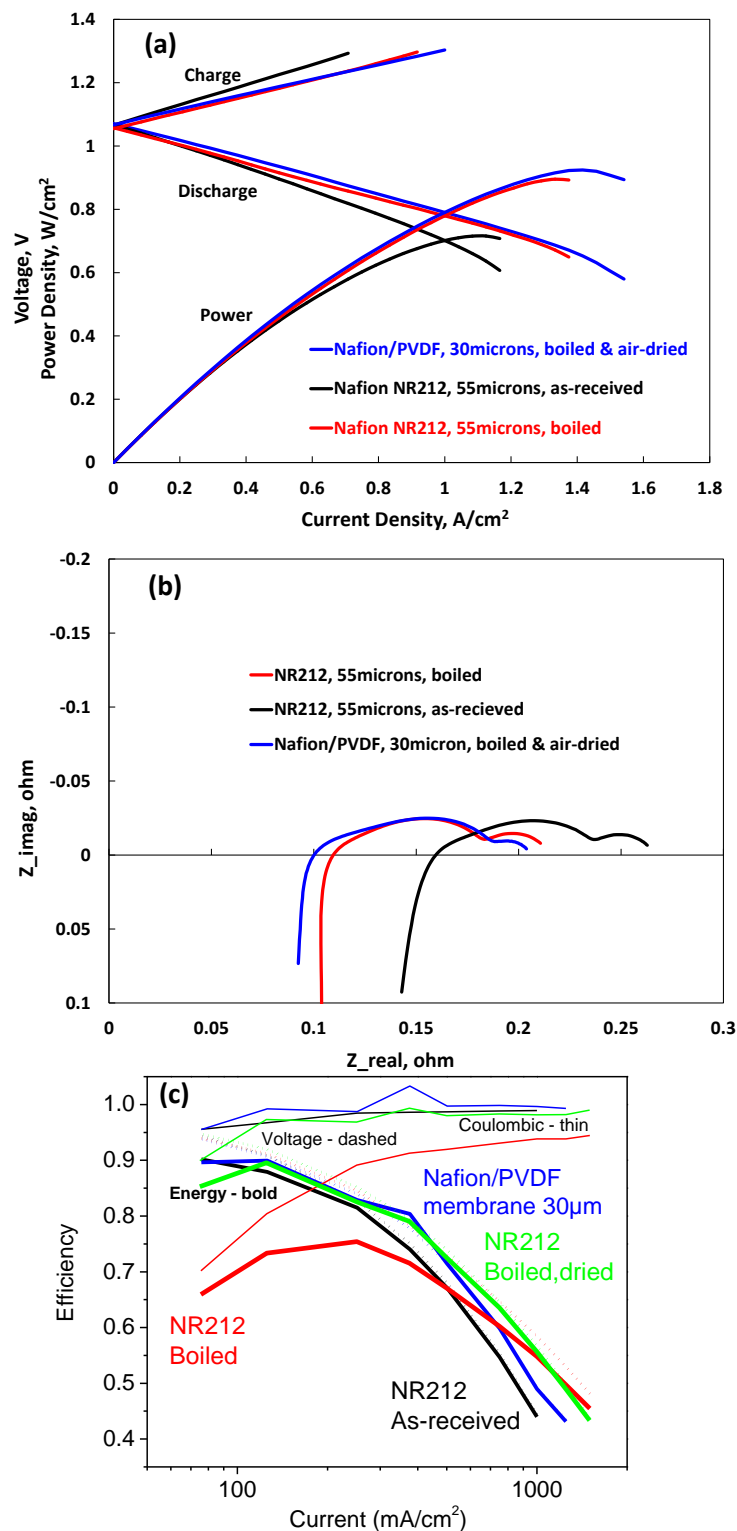**Table 2.** Cost of MEAs: new materials vs. conventional materials

Fig. 1 Nafion/PVDF performance in flow cells: a – Cell performance; b – AC impedance; c – efficiency. (H₂ electrode: Pt/C; Br₂ electrode: 3pc SGL-10AA; Solution: 1M HBr/0.9M Br₂, 20 mL/min. Thickness at as-received)
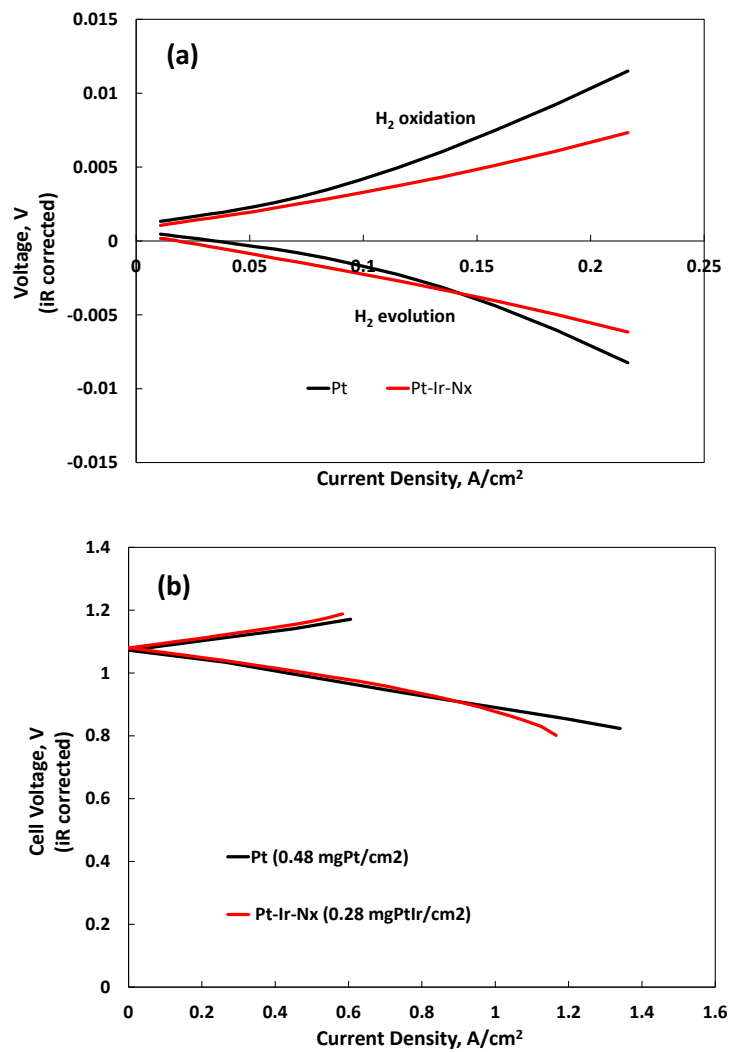
Fig. 2 Pt-Ir-N$_x$ catalyst initial performance: a- H$_2$ pump cell; b- flow cell. (Membrane: boiled NR212, not hotpressed; Br$_2$ electrode: 3pc SGL-10AA; Solution: 1M HBr/0.9M Br$_2$, 20 mL/min)
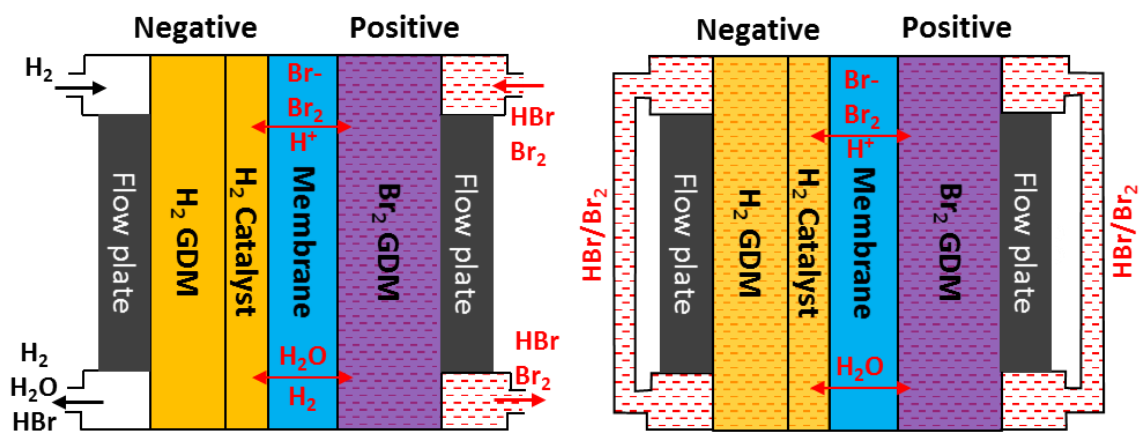
Fig. 3 Durability testing setup
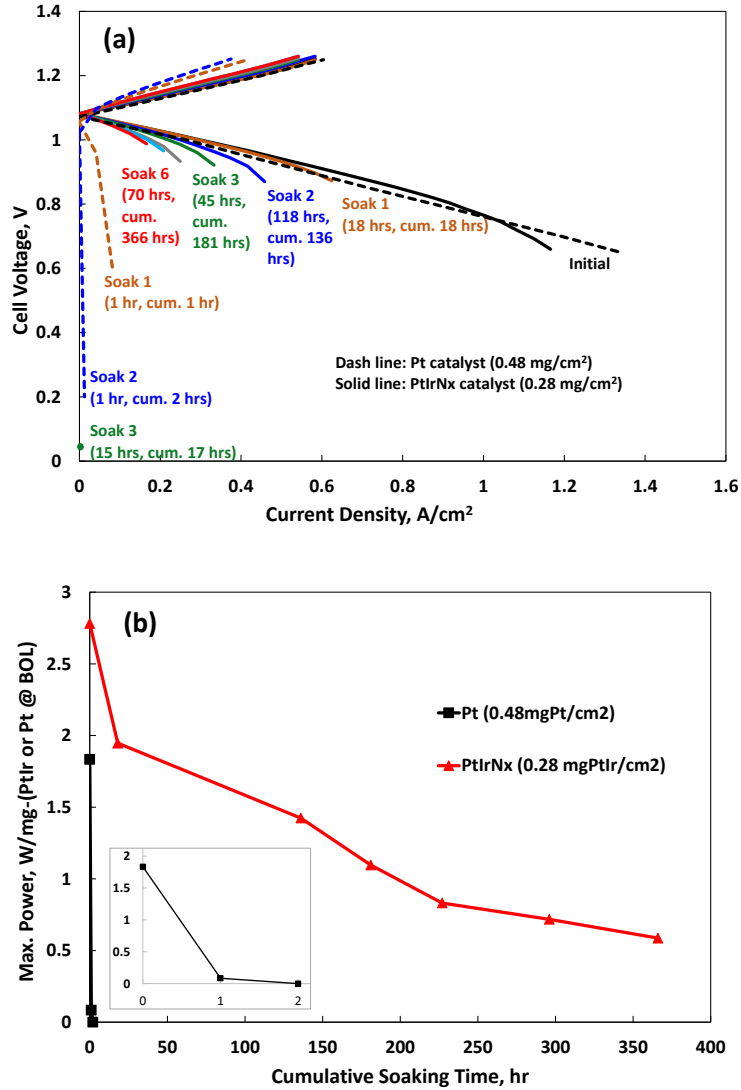(Left – setup for normal operation; Right – setup for soaking test)

Fig. 4 Pt-Ir-N$_x$ and Pt catalyst durability test (a- Polarization; b- max power normalized to initial catalyst loading. In parenthesis, first number - duration of each soak, second number - cumulative duration of soak)
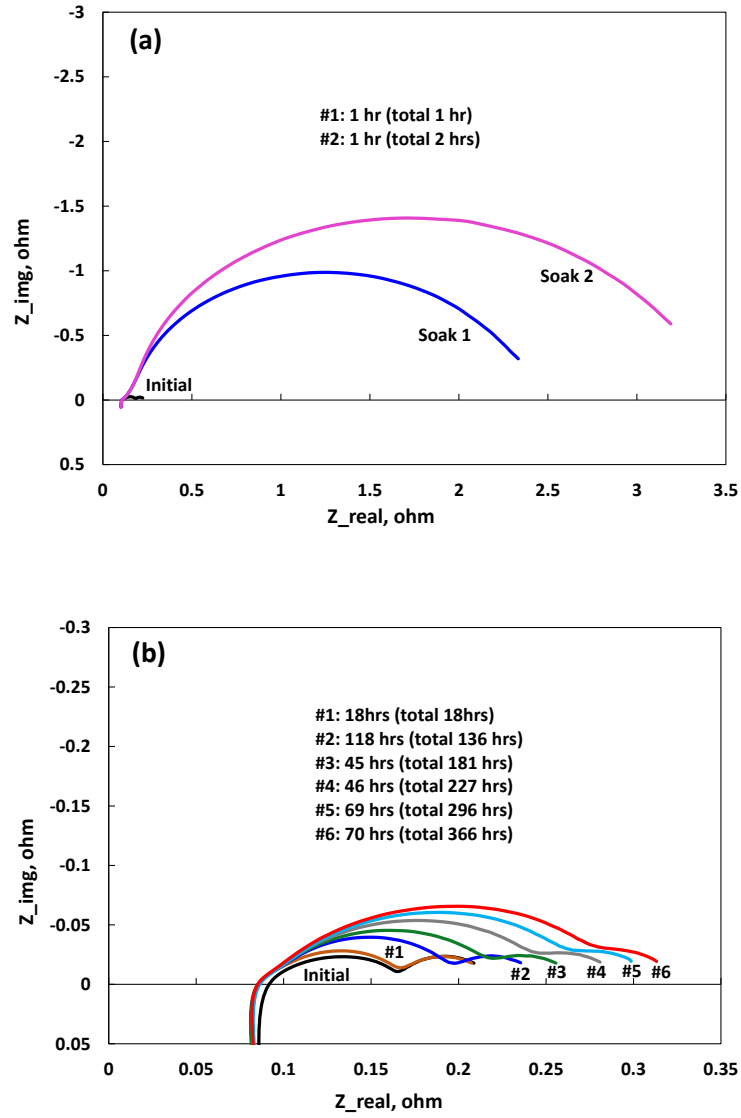
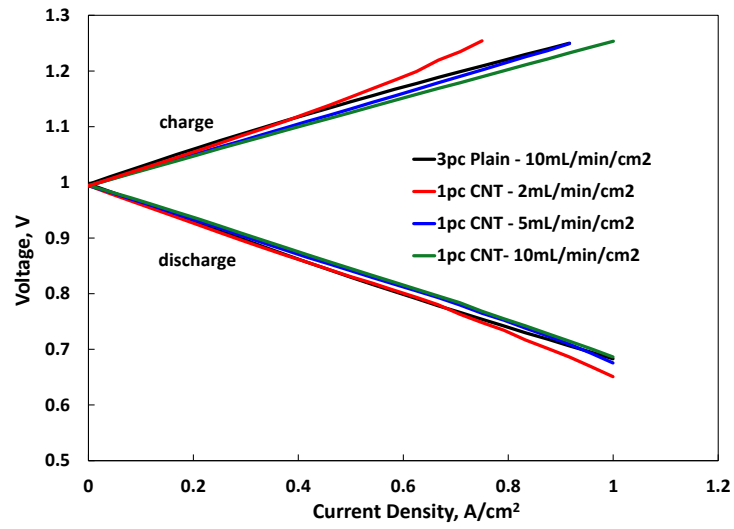**Fig. 5** AC Impedance after in-cell soaking (a- Pt; b- Pt-Ir-N$_x$)

Fig. 6 CNT Br$_2$ electrode performance in flow cells (H$_2$ electrode: Pt/C; Solution: 2M HBr/0.9M Br$_2$; Membrane: Nafion NR212, boiled)
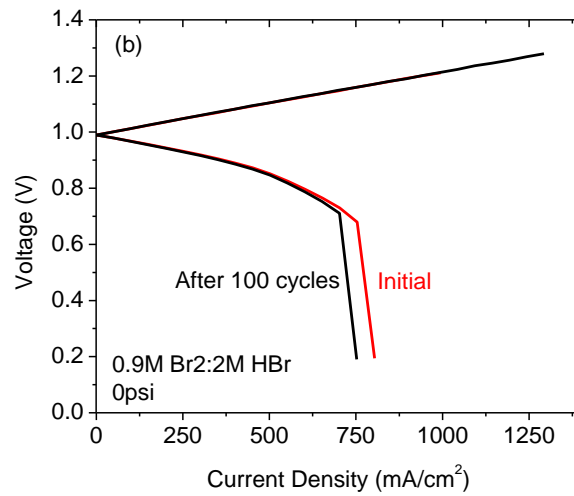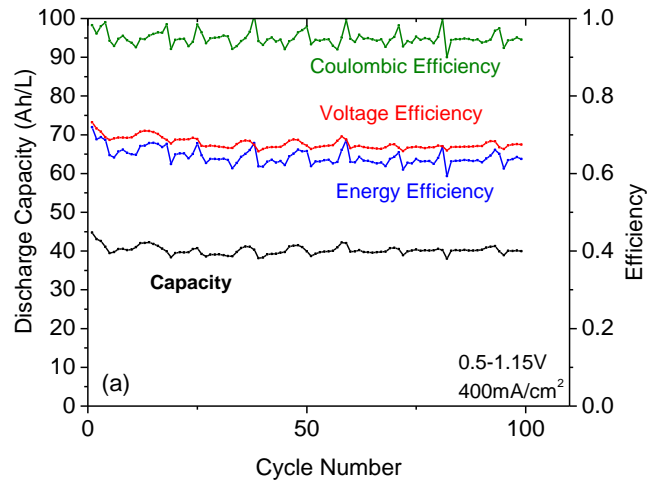
Fig. 7 Cycling test (a - capacity, efficiency; b – cell polarization performance)
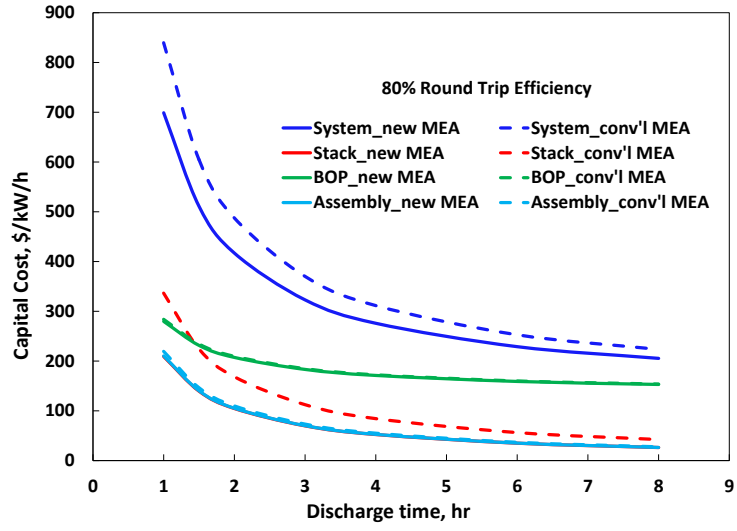Labels in Fig 7b updated to "initial" and "after 100 cycles" for clarity.

Fig. 8 H$_2$-Br$_2$ flow battery capital cost

$336/kW-hr @ 1-hr discharge

$210/kW-hr @ 1-hr discharge

Stack w/ Conventional MEAs

Stack w/ New MEAs

Gaskets & sealing 5%

Endplates & tie rods 3%

Bipolar plates 33%

Membrane 38%

Catalyst 3%

Positive GDL 8%

H2 electrode /GDL 10%

Endplates & tie rods 4%

Gaskets & sealing 8%

Membrane 21%

Catalyst 3%

Bipolar plates 45%

H2 electrode /GDL 14%

Positive GDL 5%
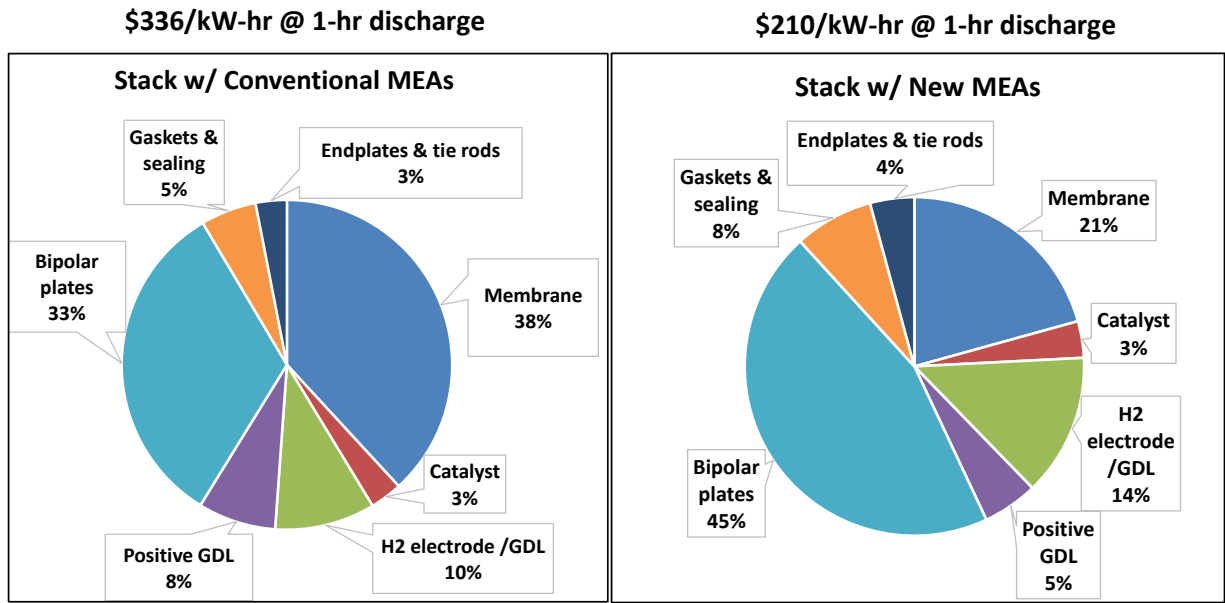
Fig. 9 Stack cost breakdown

Table 1. Membrane properties

Membrane	Conductivity mS/cm	Br Flux mg/h/cm^2	Self-Discharge mA/cm^2
NR212, as-received	66	14	1.7
NR212, boiled	149	55	12.3
Nafion/PVDF, boiled & air-dried	50	12	1.7
NR212, boiled & air-dried	97	25	3.8

Table 2. Cost of MEAs: new materials vs. conventional materials

Component	Conv'l MEA $/m^2$	New MEA $/m^2$	Cost Reduction
Membrane	350 (55μm)	140 (30μm)	60%
Catalyst	29	23	21%
Negative electrode/GDM	90	90	0%
Positive GDM	70	35	50%
MEA	**539**	**288**	**47%**